In Situ Characterisation of Pathogen Dynamics during a Pacific Oyster Mortality Syndrome Episode

Richard Marion [1, *], Rolland Jean-Luc [2], Gueguen Yannick [2], De Lorgeril Julien [2], Pouzadoux Juliette [2], Mostajir Behzad [3], Bec Beatrice [3], Mas Sébastien [4], Parin David [4], Le Gall Patrik [1], Mortreux Serge [1], Fiandrino Annie [1], Lagarde Franck [1], Messiaen Gregory [1], Fortune Mireille [1], Roque D'Orbcastel Emmanuelle [1]

[1] MARBEC, Univ Montpellier, CNRS, Ifremer, IRD, Sète, France
[2] IHPE, Univ Montpellier, CNRS, Ifremer, UPVD, Montpellier, France
[3] MARBEC, Univ Montpellier CNRS Ifremer IRD, Montpellier, France
[4] OSU-OREME, Univ Montpellier CNRS IRD IRSTEA, Sète, France

* Corresponding author : Marion Richard, email address : marion.richard@ifremer.fr

Abstract :

Significant mortality of Crassostrea gigas juveniles is observed systematically every year worldwide. Pacific Oyster Mortality Syndrome (POMS) is caused by Ostreid Herpesvirus 1 (OsHV-1) infection leading to immune suppression, followed by bacteraemia caused by a consortium of opportunistic bacteria. Using an in-situ approach and pelagic chambers, our aim in this study was to identify pathogen dynamics in oyster flesh and in the water column during the course of a mortality episode in the Mediterranean Thau lagoon (France). OsHV-1 concentrations in oyster flesh increased before the first clinical symptoms of the disease appeared, reached maximum concentrations during the moribund phase and the mortality peak. The structure of the bacterial community associated with oyster flesh changed in favour of bacterial genera previously associated with oyster mortality including Vibrio, Arcobacter, Psychrobium, and Psychrilyobacter. During the oyster mortality episode, releases of OsHV-1 and opportunistic bacteria were observed, in succession, in the water surrounding the oyster lanterns. These releases may favour the spread of disease within oyster farms and potentially impact other marine species, thereby reducing marine biodiversity in shellfish farming areas.

Highlights

► An increase in OsHV-1 and opportunistic bacterial pathogens occurs in oyster flesh during a POMS outbreak ► OsHV-1 and opportunistic bacteria are released, in succession, into surrounding water ► Viral and bacterial pathogen release was at a maximum during the moribund and mortality phases of the outbreak

Keywords : Crassostrea gigas, aquaculture, disease, Ostreid Herpesvirus 1, microbiota, bacteria, Thau lagoon

36   **1. Introduction**

37   Since 2008, from 40% to 100% *Crassostrea gigas* juveniles in oyster cultures have been

38   decimated annually by Pacific Oyster Mortality Syndrome (POMS) (Garcia et al., 2011;

39   Pernet et al., 2012; Segarra et al., 2010). Pacific Oyster Mortality Syndrome is now reported

40   worldwide (Carrasco et al., 2017; Mineur et al., 2014; Paul-Pont et al., 2014). Together with

41   OsHV-1, *Vibrio splendidus* has also been implicated as a possible pathogen for oyster

42   juveniles (Pernet et al., 2012; Petton et al., 2015b). Using a laboratory-based approach, de

43   Lorgeril et al. (2018) demonstrated that POMS is caused by OsHV-1 infection leading to

44   immune suppression, followed by bacteraemia caused by a consortium of opportunistic

45   bacteria including those belonging to the *Vibrio, Arcobacter, Psychromonas, Psychrobium,*

46   and *Marinomonas* genera. As specified by King et al. (2019), the challenge is now to

47   demonstrate "how the oyster microbiome responds before, during and after an environmental

48   disease outbreak".

49   Although many studies have explored disease-controlling factors (Petton et al., 2015a,

50   2013; Whittington et al., 2015a) and the consequences of infection for oysters (Corporeau et

51   al., 2014; Green et al., 2016, 2015; Tamayo et al., 2014), few have investigated the

52   consequences of these mortality events for the environment. Indeed, unlike in most other

53   animal production industries, sick and dead individuals are not separated from conspecifics in

54   shellfish farms, but remain in the rearing environment until their flesh totally disappears

55   (Richard et al. 2017, 2019). The mortality of oyster juveniles has been shown to increase

56   ammonium and phosphate fluxes at the oyster interface (Richard et al., 2017) and to reduce

57   the N/P ratio due to decomposition of the flesh (Richard et al., 2019, 2017). Oyster mortality

58   has been also shown to induce changes in microbial planktonic components during the

59   infection and mortality peak, with proliferation of picophytoplankton and heterotrophic

60   ciliates (*Balanion, Uronema*) (Richard et al., 2019). Ciliates may proliferate in response to a

61 bacterial proliferation associated with decaying oyster tissue (Richard et al., 2019). Beyond

62 disturbing the ecosystem, the fact sick and dead individuals remain in the environment could

63 also favour cross-contamination and disease spread. Indeed, oyster mortality shows strong

64 spatial dependence, starting inside the oyster farm and rapidly spreading beyond (Pernet et al.,

65 2014a). We propose the hypothesis that pathogens released from infected and dead oysters

66 into the water column may be at the origin of disease transmission to naïve oysters, as already

67 shown using a laboratory-based approach with OsHV-1 (David Schikorski et al., 2011). To

68 date, no *in-situ* description or quantification is available in the literature on potential pathogen

69 releases during mortality events in ecosystems where shellfish are cultured.

70 Using an *in-situ* approach in the natural environment, the aim of this study was to

71 demonstrate, (i) temporal OsHV-1 dynamic and microbiota community changes in oyster

72 flesh and (ii) the release of OsHV-1 and opportunistic bacteria from oysters into the water

73 column, before, during and after an oyster mortality episode in the Mediterranean Thau

74 lagoon. These data will advance our understanding of the consequences of the massive and

75 recurrent POMS events for the dynamics of potential pathogens in ecosystems where shellfish

76 are cultured.

77

78 **2. Material and methods**

79 *2.1. Experimental design and devices*

80 As described in the paper by Richard et al. (2019), the experiment was conducted from

81 March to June 2015 in the Thau Lagoon on the French Mediterranean coast (43°22'44.87''N,

82 3°34'37.64'E). At the end of March 2015, 27,000 juvenile oysters were purchased from

83 SCEA Charente Naissains (Port des Barques, France). The juveniles originated from the

84 Marennes-Oléron area (45°58′16.08″N, 01°06′16.2″W), where they were collected on spat

85 collectors in July 2014 and grown until being harvested and shipped to the study site at Sète

86 for the experiment. Mean total wet weight (WW) and length (± SD) measured on arrival at the

87 laboratory were 0.49 ± 0.02 WWg and 1.8 ± 0.02 cm, respectively. After two days of

88 acclimation in laboratory tanks, the juvenile oysters were placed in eighteen lantern nets (Ø:

89 45 cm, H: 105 cm) comprised of seven shelves at a stocking density of 100, 200, 350

90 individuals per shelf. The 18 lanterns of oyster juveniles were then suspended from an

91 experimental structure (called a table) and immersed one metre below the surface of Thau

92 Lagoon (Figure 1). The water depth at the site was 4 m.

C) Water was sampled in the pelagic chamber using a tube and a peristaltic pump

Water was pumped using a tube at T0 and Tf

The top of the chamber was closed with a waterproof cap lid

B) Each lantern was incubated in a pelagic chamber for 5 hours

The chamber was placed positioned so it surrounded the lantern

A) The oysters were counted and sampled

93
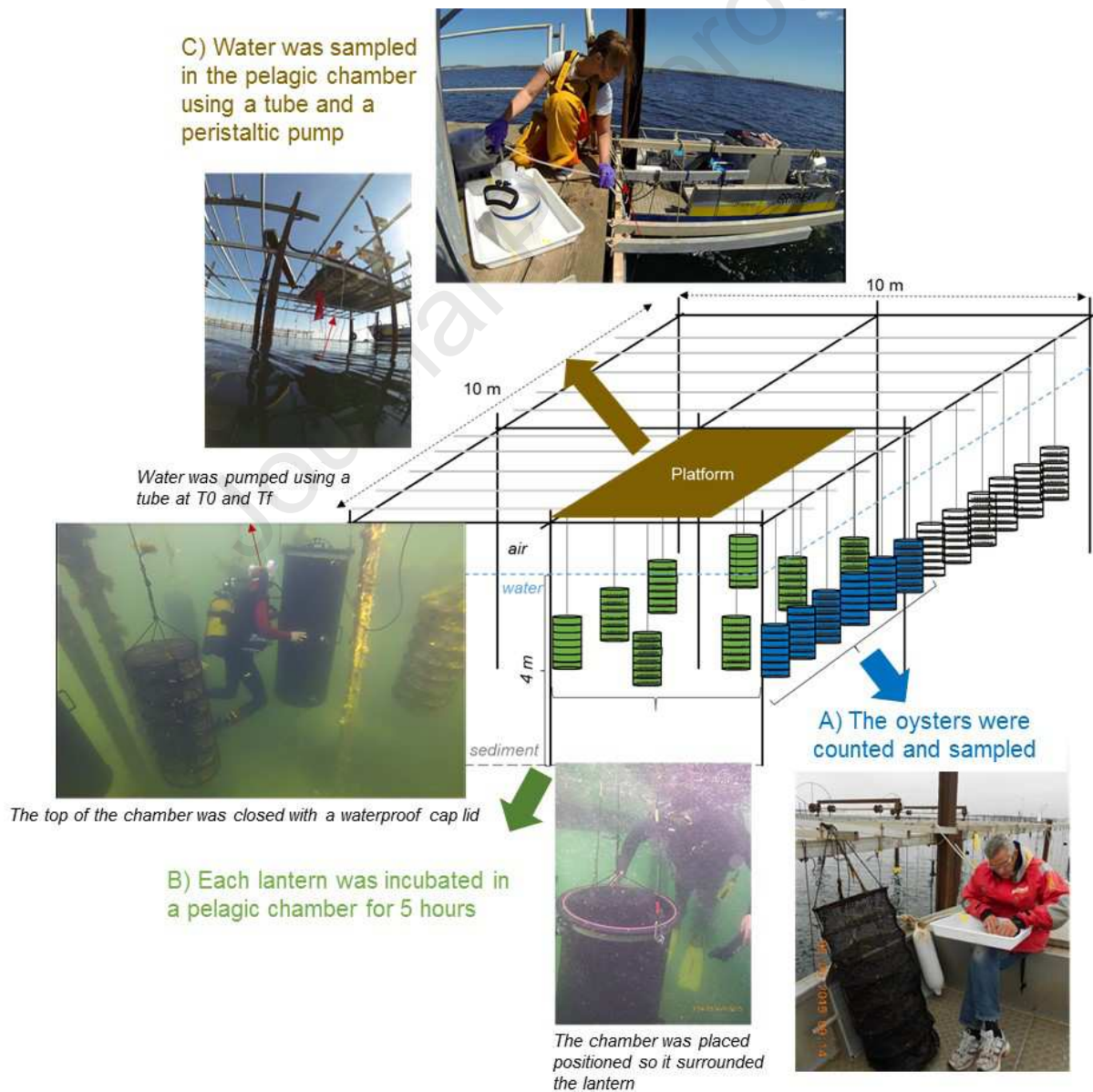
94   Figure 1: Schematic drawing of the experimental "table" and location of the different

95   batches of lanterns used for evaluation A) Mortality rate and pathogen dynamics in oyster

96   flesh (blue batch) and B) Pathogen dynamics in the water column and releases using the

97   pelagic chamber (green batch). Photographs illustrating A) oyster sampling, B) how the

98   lantern is incubated in the pelagic chamber, and C) water being pumped into the pelagic

99   chamber.

100

101   A first batch of six lanterns was randomly chosen and used to study oyster juvenile

102   mortality and pathogen dynamics in oyster flesh (Figure 1A, Figure 2A). The lanterns in this

103   batch were randomly distributed in the right-hand part of the table so as to be accessible by

104   boat (Figure 1A). A second batch of six lanterns of oyster juveniles and two empty lanterns

105   were randomly selected and used to estimate pathogens dynamics and releases into the water

106   column using pelagic chambers (Figure 1B, Figure 2B). The lanterns were randomly located

107   in the first (5 x 5 m) squares of the table (Figure 2B). Different batches of lanterns were

108   sampled for Tasks A and B (Figures 1, 2) because in Task A, the lanterns had to be removed

109   from the water and placed in the boat for oyster sampling and counting, which probably

110   dispersed decaying flesh and faeces. The lanterns for Task B were left in the water to limit

111   physical disturbance and possible dispersal of decaying oysters and faeces so that the release

112   of pathogens during the decomposition of the flesh could be measured in real conditions. The

113   other six lanterns of oysters were placed near the first batches but were not sampled. These

114   were used to maximise our chances of observing changes in the water column linked to oyster

115   mortality. The abundance of oyster juveniles used in this study (27,000 ind. per 100m², see

116   figure 2 for details of the area: 270 ind.m^2) was lower than in shellfish farms where 1,200

117   lanterns containing 350 individuals per storey were suspended per culture table (1,200 x 350 x

118 7: 2,940,000 ind. per 500 m²: ie. 5880 ind.m^2, see figure 2 in Gangnery et al. 2003 for details

119 of the size and structure of a standard culture table in the Thau lagoon).

120

121

A) Mortality rate and pathogen dynamics in oyster flesh
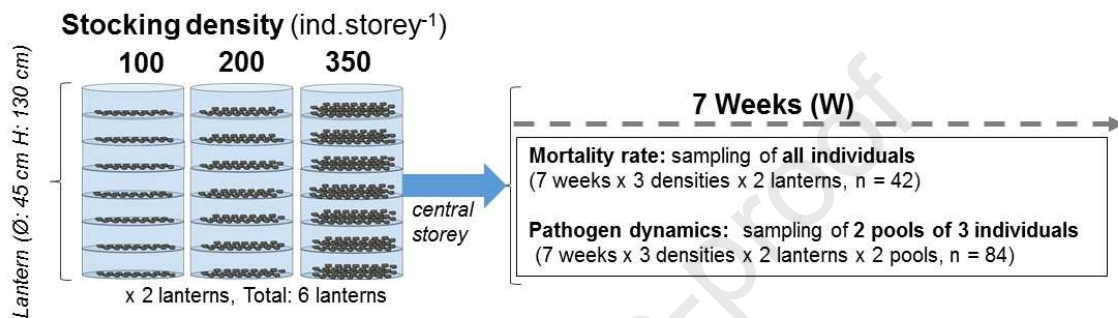
B) Pathogen dynamics in the water column and pathogen releases
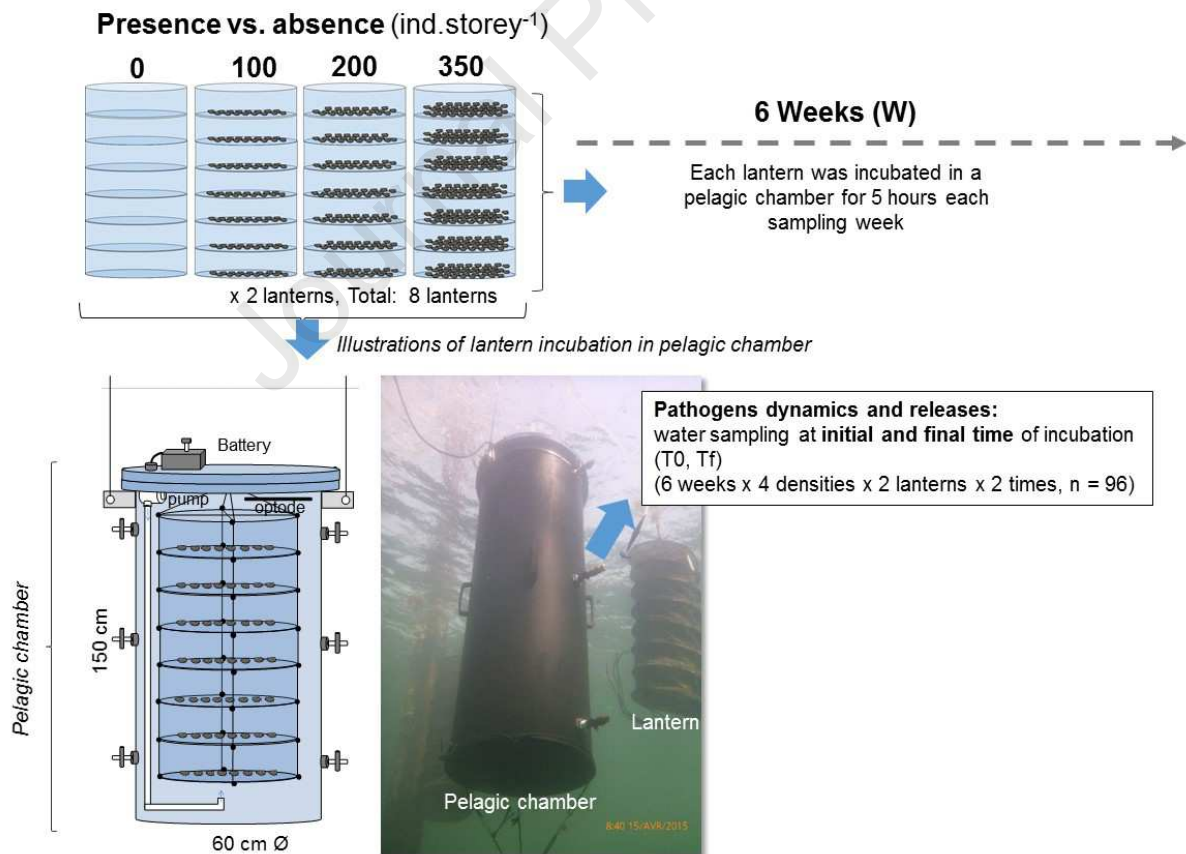
122

123 Figure 2: Experimental designs to evaluate A) Mortality rate and pathogen dynamics in

124 oyster flesh and B) Pathogen dynamics in the water column and releases. Experimental

125   designs were conducted with 3 or 4 stocking densities (0, 100, 200, 350) to assess absence (0)

126   vs. oyster presence or density (100, 200, 350) over 7 or 6 weeks, depending on the parameter

127   studied (A or B respectively). To estimate pathogen dynamics and releases, the eight lanterns

128   (0, 100, 200, 350) were incubated one a week for 5 hours using four pelagic chambers over

129   two days, at a rate of 4 incubations per day. Water was sampled at 2 time points during the

130   incubation: at the initial (T0) and at the final time point (Tf: *i.e.* after 5 hours). The diagram

131   and photo illustrate a pelagic chamber composed of a cylindrical tube, a waterproof cap, a

132   water circulation system driven by an independent pump and an oxygen optode probe.

133   Modified from Richard et al. (2019)

134

135   *Task A: Oyster juvenile mortality and pathogen dynamics in oyster flesh*

136   Throughout the experiment, on the central shelf, the numbers of living, dead, and

137   moribund oysters in two lanterns per stocking density were counted at weekly intervals

138   (Figure 1A). As described in Richard et al. (2019), oysters were qualified as (i) dead, when

139   their valves were open at emersion; (ii) alive, when their valves were closed at emersion; or

140   (iii) moribund, when their valves did not close properly and air bubbles escaped when

141   pressure was exerted on the two valves. Dead oysters were removed from the sampled shelf at

142   each sampling point. "Instantaneous" rates of mortality and moribund oysters were calculated

143   each week from the number of dead or moribund individuals on the shelf relative to the total

144   number of oysters observed. Cumulative mortality rates were calculated each week from the

145   sums of dead oysters observed from the beginning of the experiment to the initial number of

146   oysters per shelf. These data were used to identify different steps of the mortality episode

147   termed "before", "starting", "moribund", "mortality" and "post-mortality". In parallel, each

148   week, two batches of three oysters were randomly sampled on the central shelf of each lantern

In situ microbial dynamics during POMS

149   for OsHV-1 and microbiota analysis (7 weeks x 3 densities (100, 200, 250) x 2 lanterns x 2

150   batches, n = 84) (Figure 2A).

151

152   *Task B: Pathogen dynamics in the water column and releases*

153   At weekly intervals before, during, and after the mortality event, four 425-L pelagic

154   chambers (150 cm Height, 60 cm Ø, Fig. 2B) were positioned by divers around two sets of

155   four lanterns either containing no oysters (0: absence), or 100, 200, or 350 oysters (presence:

156   Fig. 2B). During placement, pelagic chambers were first delicately positioned around each

157   lantern (Figure 1B). Next, the pelagic chambers were closed at the top with a waterproof cap

158   (Figures 1B, 2B). There was only one lantern per pelagic chamber as shown in Figure 1 and

159   described in Fig. 2B. The principle behind incubation in the pelagic chambers was to enclose

160   the oysters in a closed system without water renewal. Over time, the oysters would consume

161   the available oxygen via respiration, and the oxygen concentration would consequently

162   decrease. Using this confinement, we were able to measure the exchanges at the interface of

163   the oyster lanterns and determine what is consumed (e.g., phytoplankton), excreted (e.g.,

164   ammonium, phosphates) or released (e.g., pathogens). To be able to measure these fluxes, the

165   incubation time had to be long enough to induce significant variability of the concentrations

166   observed at the beginning and end of incubation without stressing the oysters. In this study,

167   incubation was limited to five hours to enable measurement of significant pathogen releases

168   without causing physiological stress to the juvenile oysters. Oxygen depletion did not exceed

169   20% and oxygen levels always remained above 70% according to the values recorded by each

170   of the HOBO U26 Dissolved Oxygen loggers (Figure 1B). Water was sampled from each

171   pelagic chamber at the beginning and end of the five-hour-incubation period (T0, Tf; Figure

172   1B, 2B) at each stocking density and in each sampling week for the analysis of OsHV-1 and

173   microbiota analysis in the water column. The water was sampled in the pelagic chamber using

174   a tube, a peristaltic pump and a series of plastic bottles (previously cleaned with 1N

175   chlorhydric acid), from a platform as shown in Figure 1C. At the end of the incubation, the

176   pelagic chambers were removed and placed in the boat, then, back at the laboratory, were

177   cleaned, and stored until the following sampling session. Each sampling week in 2015 was

178   attributed a number (W16 to W22). W16 corresponded to the 13-19th of April, W17 to the 20-

179   26th of April, W18 to 27th of April-3rd of May, W19 to 4-10th of May, W20 to 11-17th of May,

180   W21 to 18-24th of May, and W22 to 25-31st of May, 2015.

181

182   *2.2. Sampling*

183   *Oysters*

184   Oyster juveniles were transported to the lab in coolers. They were measured with a calliper

185   and weighed to 10^{-3} g on a precision balance. They were dissected. Two batches, comprising

186   the flesh of three oysters were randomly combined in two Eppendorf tubes to produce two

187   samples per lantern for DNA extraction. The Eppendorf tubes were filled with 100% ethanol

188   and stored at -20 °C.

189

190   *Water*

191   The water samples were transported to the lab in plastic bottles in coolers. Water samples

192   (500 ml) taken at T0 and Tf, were vacuum filtered using 0.22 µm (Acetate Plus) membranes

193   to dissociate free forms of OsHV-1 from those associated with living and non-living particles.

194   The membranes were placed in Eppendorf tubes filled with 100% ethanol and kept at -20 °C.

195   The 0.22 µm-filtered water samples were placed in 50-ml sterile tubes and kept at -20 °C. The

196   samples taken at T0 in the absence of oysters (0) were used to describe the dynamics of

197   OsHV-1 and microbiota in the water column over time (6 weeks x 2 lanterns, n = 12). The

198   samples taken at Tf were used to compare and quantify changes in OsHV-1 levels and

199   microbiota composition in the water in the pelagic chamber in the presence and in the absence

200   of oysters over time (5 weeks (no Tf data in W16) x 4 densities (0, 100, 200, 350) x 2

201   lanterns, n = 40).

202   Quantification of OsHV-1 and microbiota analyses were conducted from common DNA

203   extractions of the same samples of oyster flesh and water.

204

205   *2.4. Nucleic acid extraction*

206   Environmental DNA from the filters was extracted and purified using the standard

207   current molecular biology protocols described in unit 2.2.1 (Ausubel et al., 2003). Total DNA

208   from oyster tissues was extracted and purified using the Wizard® SV Genomic DNA

209   Purification System (Promega). Briefly, using a pellet mixer, oyster flesh samples were

210   homogenised on ice in a 1.5-mL microtube containing a digestion solution (10 mM Tris-Base,

211   pH 8, 100 mM NaCl, 25 mM EDTA dihydrate, 0.5 % SDS, 0.1 mg/mL proteinase K), and

212   then incubated at 55 °C overnight. The remaining oyster tissues were centrifuged at 2,000 *g*

213   for 2 min and DNA was extracted from the supernatant according to the manufacturer's

214   instructions. After purification, the DNA from the oyster tissues and filters was kept in 100

215   µL of DNAse/RNAse-Free distilled water at -20 °C until qPCR and 16S rDNA barcoding.

216   The concentration and purity of the DNA were checked with a Nanodrop ND-1000

217   spectrometer (Thermo Scientific).

218

219   *2.5. Quantification of OsHV-1*

220   Ostreid herpesvirus type 1 genomic DNA was detected and quantified using quantitative

221   PCR (qPCR). A LightCycler® 480 System (Roche) was used for qPCR with the following

222   programme: enzyme activation at 95 °C for 10 min, followed by 40 denaturation cycles (95

223   °C, 10 s), hybridisation (60 °C, 20 s) and finally elongation (72 °C, 25 s). The PCR reaction

224   volume used was 6 µL. Each volume contained LightCycler 480 SYBR Green I Master mix

225   (Roche), 100 nM of pathogen-specific primers and 1 µl of 100 ng sample DNA. Pathogen-

226   specific primer pair sequences were as follows: C9: 5'-GAG GGA AAT TTG CGA GAG

227   AA-3', sense and C10: 5'-ATC ACC GGC AGA CGT AGG-3', antisense (Pépin et al.,

228   2008). Subsequently, an amplicon melting temperature curve was generated to check the

229   specificity of the amplification products. The absolute number of viral DNA copies was

230   estimated by comparing the observed Cq values to a standard curve of the DP amplification

231   product cloned into the pCR4-TOPO vector for OsHV-1 (Lafont et al., 2017). Viral DNA

232   copy numbers were reported with respect to sampled flesh weight and filtered water volume

233   expressed per g^{-1} or mL^{-1}.

234   Variations in OsHV-1 DNA copies over time were calculated based on the absence

235   (Equation 1) and presence of oyster juveniles (Equation 2) according to the following

236   equations where V corresponds to the volume of the chamber (425 L):

237   (1) Absence: $(\text{CopiesC9C10.lantern}^{-1}. h^{-1})$ = ([0 : absence]Tf –[0 : absence]T0)/(Tf-T0) x

238   V

239   (2) Presence: $(\text{CopiesC9C10.lantern}^{-1}. h^{-1})$ = ([presence]Tf – [absence]T0)/(Tf-T0) x V

240

241   *2.6. Analysis of bacterial microbiota*

242   For each sample, 16S rDNA amplicon libraries were generated using the 341F-

243   CCTACGGGNGGCWGCAG and 805R-GACTACHVGGGTATCTAATCC primers

244   targeting the variable V3-V4 loops for bacterial communities (Klindworth et al., 2013).

245   Before the library was constructed, DNA was purified a second time using the Macherey-

246   Nagel tissue kit (reference 740952.250) according to the manufacturer's instructions. Paired-

247   end sequencing with a 250-bp read length was performed at the "Bio-Environnement" UPVD

248   technology platform (University of Perpignan Via Domitia Perpignan, France) on a MiSeq

249   system (Illumina) using v2 chemistry according to the manufacturer's protocol. The FROGS

250   pipeline (Find Rapidly OTU with Galaxy Solution) implemented on a galaxy instance was

251   used for data processing (Escudié et al., 2018). In brief, paired reads were merged using

252   FLASH (Magoč and Salzberg, 2011). After denoising and primer/adapter removal with

253   Cutadapt (Martin, 2011), clustering was performed with SWARM, which uses a clustering

254   algorithm with a threshold (distance =3) corresponding to the maximum number of

255   differences between two OTUs (Mahé et al., 2014). Chimeras were removed using

256   VSEARCH (Rognes et al., 2016). The dataset was filtered for sequences present in minus in 3

257   samples and the remaining data were rarefied to allow for even coverage across all samples.

258   We then produced affiliations using BLAST against the Silva 16S rDNA database (release

259   132, Dec 2017) to produce an OTU and affiliation table in the standard BIOM format.

260   Rarefaction curves of the species richness were generated using the R package and the

261   rarefy_even_depth and ggrare functions (McMurdie and Holmes, 2013). We used phyloseq

262   for community composition analysis, to infer alpha diversity metrics at the OTU level, as well

263   as beta diversity (between sample distance) from the OTU table. Community similarity was

264   assessed by principal coordinate analysis (PCoA) using the Bray-Curtis dissimilarity.

265

266   *2.7. Statistical analyses*

267   PERMANOVA was used to test the influence of the sampling week and of the density and

268   their interaction (Week x Density) on mortality rates and OsHV-1 concentrations in oyster

269   flesh and in the water column. Given that oyster density (100, 200, 350) was not found to

270   affect mortality rates and OsHV-1 concentrations in oyster flesh and the water column, the

271   effect of week, oyster presence (0: absence vs. presence: 100, 200, 350) and their interactions

272   (Week x Presence) on OsHV-1 fluxes were tested to demonstrate the effect of oysters on

273   OsHV-1 and bacteria releases. *A posteriori* tests were performed to compare individual means

274   with each other when significant variations were observed. Analyses were performed with

275   JMP and PRIMER software, and the PERMANOVA package (Plymouth Routines in

276   Multivariate Ecological Research (Clarke and Warwick, 2001).

277   Principal coordinate analyses (PCoA, {phyloseq}) were computed to represent

278   dissimilarities between samples using the Bray-Curtis distance matrix. We used DESeq2

279   (Love et al., 2014) to identify candidate taxa (OTU rank) with changes in abundances

280   between the initial and different time points of the kinetics (Tf vs. T0 each week for water and

281   W17 to W20 vs. W16 for oyster flesh). Heatmaps of genera with significant changes in

282   abundances were then computed using relative abundances and Multiple Array Viewer

283   software.

284

285   **3. Results**

286   *3.1. Mortality kinetics*

287   As already described by Richard et al. (2019), mortality of juvenile oysters occurred in the

288   Thau lagoon between April and May 2015 (Figure 3A). Instantaneous rates of mortality and

289   of moribund oysters varied significantly with the week (p = 0.001, n = 42), but not with the

290   density (moribund p = 0.6, mortality p = 0.9, n = 42) or "week x density" interactions

291   (moribund p = 0.9, mortality p = 0.4, n = 42). The number of moribund oysters (32 ± 3%)

292   peaked in week 18 (Figure 3A) one week before the highest mortality rate was reached in

293   week 19 (32 ± 5%: Figure 3A). These weeks were thus categorised as "moribund" and

294   "mortality" stages, respectively. At the end of the event (W22), the cumulative mortality rate

295   reached $54.2 \pm 1.1\%$. Based on these results, different periods related to oyster mortality were

296   defined as follows: "before" (W16) "starting" (W17), "moribund" (W18), "mortality peak

297   (W19), "post-peak" (labelled 1, 2, 3 for W20, 21 and 22, respectively; Figure 3).
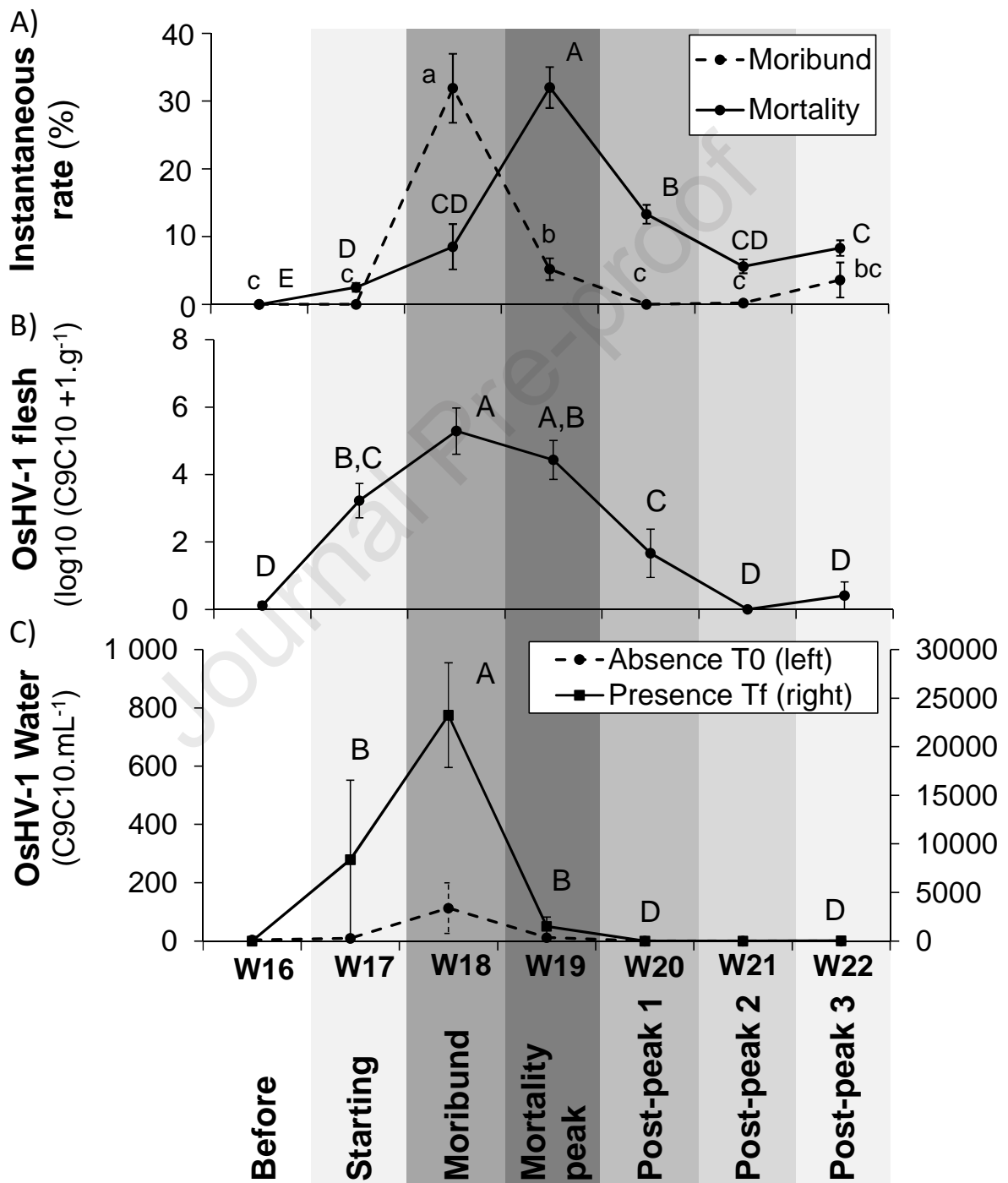
298

299   Figure 3: A) Mean (± SE Standard Error) instantaneous moribund and mortality rates

300   (from Richard et al. 2019), B) OsHV-1 concentrations in oyster flesh (copies.g-1) and C) in

301   the water column (i.e. associated with > 0.2 µm-Suspended Particulate Matter SPM,

302   copies.mL^{-1}), observed in absence of oysters at the start of incubation (T0: values are on the

303   left axis) and in the presence of oysters at the final incubation time point (Tf: values are on the

304   right axis), according to the sampling week (W16: 13–19th of April, W17: 20–26th of April,

305   W18: 27th of April-3rd of May, W19: 4–10th of May, W20: 11–17th of May, W21: 18–24th of

306   May and W22: 25–31st of May 2015). Different letters indicate significant differences among

307   weeks.

308

309   *3.2. Dynamics of OsHV-1 in oyster flesh and in the water column*

310   Concentrations of OsHV-1 [flesh] (log10 (x+1)) varied significantly according to week and

311   density interactions (p = 0.002) with no significant variation observed among density during

312   W16, W18, W19 and W21, but with higher means for the 100 density in W17 and W20.

313   Significant variations in OsHV-1 [flesh] over time were observed within densities. Mean

314   OsHV-1[flesh] dynamics preceded the mortality dynamics (Figure 3B). Concentrations of

315   OsHV-1[flesh] (copies.g^{-1}) started to increase from W17 (8.9 x 10^{+04}), during the "starting"

316   period, and reached maximum levels at the "moribund peak" (W18: 1.09 x 10^{+07} copies.g^{-1}),

317   before decreasing from W19 (7.1 x 10^{+06} copies.g^{-1}) to W20 (7.79 x 10^{+04}) and becoming

318   undetectable in W21 (Figure 3B; Appendix C).

319   OsHV-1 was quantified in the water column, i.e. associated with living and non-living

320   particles (Suspended Particulate Matter SPM > 0.22 µm), but was not detected in the free

321   form (i.e., in 0.22 µm-filtered water) (Appendix D). The highest mean amount of OsHV-1

322   [SPM > 0.22 µm] in the absence of oyster (0, T0) was observed in W18 (112.5 ± 86.8

323   copiesC9C10.mL^{-1}, Figure 3C), but the temporal dynamics were nevertheless not significant

324   (n=12, p = 0.062). OsHV-1 amounts [SPM > 0.22 µm] increased during the 5-h incubation

325   period in the presence of oysters in the pelagic chambers. Mean OsHV-1 amounts [SPM >

326   0.22 µm] in the presence of oysters and at the final time point ranged from 1,503 to 23,251

327   C9C10 copies.ml^{-1} between W17 and W19, with the highest mean observed in W18 (Figure.

328   3C). Positive fluxes of OsHV-1 DNA copies (C9C10 copies) were observed in the pelagic

329   chambers in presence of oysters, corresponding to the release of OsHV-1 DNA copies from

330   oysters into the surrounding water. Release of OsHV-1 varied significantly according to

331   "oyster presence and week" interactions (p = 0.001, n = 38), with higher means observed in

332   the presence than in the absence of oysters in W18 and W19 (*: Figure 4). Release of OsHV-1

333   DNA started in W17, and the highest mean was reached in W18 with $2.1 \pm 0.5 \times 10^9$ copies

334   OsHV-1.oyster lantern^{-1}.h^{-1}. In W19, OsHV-1 release was still significant, but lower, while no

335   significant OsHV-1 release was observed in W20 and W22 (Figure 4). Fluxes of OsHV-1

336   DNA were positively correlated with the concentrations observed in oyster flesh ($R^2 = 0.4$; p

337   < 0.001, n = 28).
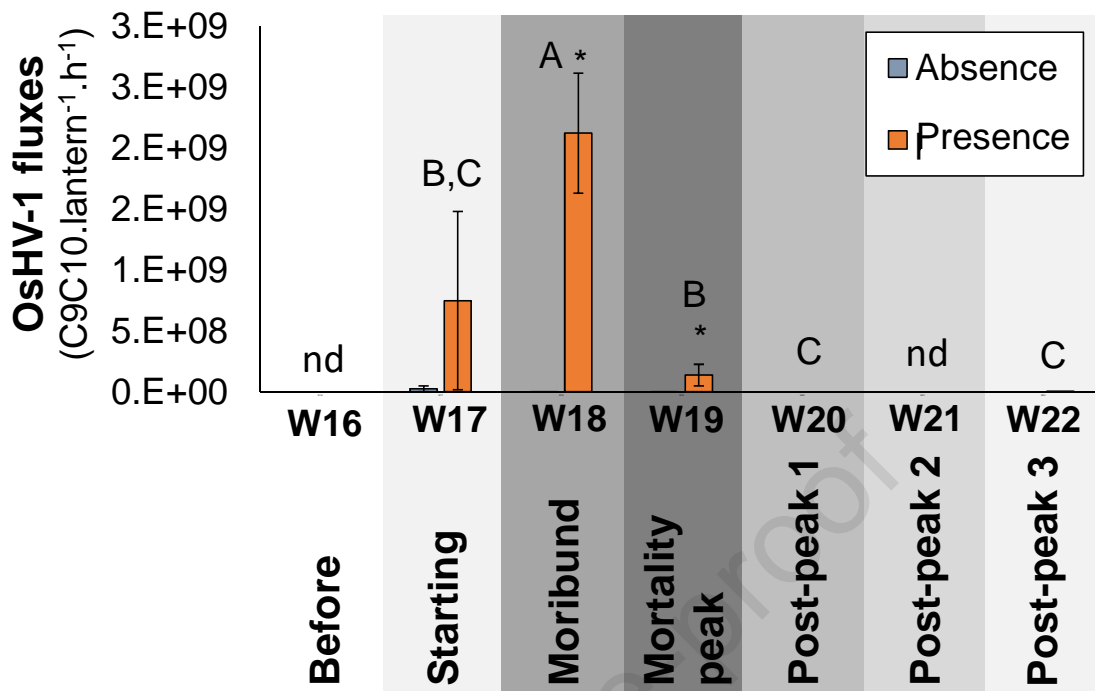
Figure 4: Mean (± SE) OsHV-1 releases from the lanterns into the surrounding water column in presence or absence of oysters according to sampling weeks (W16: 13–19th of April, W17: 20–26th of April, W18: 27 April-3rd of May, W19: 4–10th of May, W20: 11–17th of May, W21: 18–24th of May and W22: 25–31st of May 2015). Different letters indicate significant differences between weeks in the presence of oysters. Stars indicate significant differences according to the absence/presence of oysters in a given week.

3.3. Dynamics of bacterial microbiota in oyster flesh and in the water column

To investigate the dynamics of the oyster flesh and water column microbiota during the disease episode, we analysed total bacterial communities using 16S metabarcoding over the six weeks of the experiment. A total of 7,011,267 reads were obtained from 142 libraries (Appendix A, B). After the cleaning steps and filtering, 5,009,278 sequences corresponding to 8,391 OTUs were kept for further analyses (Appendix A, B). Notably, the 100 most abundant

352   OTUs accounted for more than 75% of all the sequences. Microbiota OTU richness assessed

353   by a Chao1 index was higher in the sea water samples than in the oyster flesh samples

354   (Anova, d.f.=1, p < 2e-16; Figure 5A). In addition, the Shannon microbiota alpha diversity

355   index was also significantly higher in water samples (Anova, d.f.=1, p <2e-15; Figure 5A),

356   demonstrating that bacterial diversity in sea water was higher than in oyster flesh. Class-level

357   assignment of bacterial OTUs indicated dominance of *Gammaproteobacteria* in oyster flesh

358   samples, whereas the dominant classes in the water samples were *Alphaproteobacteria*,

359   *Actinobacteria* and *Bacteroidia* (Figure 5B). Lastly, principal coordinate analysis based on the

360   Bray-Curtis dissimilarity index showed partitioning of bacteria (Multivariate Anova, pvalue

361   <1e-04) into communities originating from water or from oyster flesh (Figure 5C), whereas

362   no partitioning was observed according to density in water (Multivariate Anova, pvalue =

363   0.12) or in oyster flesh ((Multivariate Anova, pvalue =0.36). Taken together, these results

364   demonstrate a difference in the bacterial microbiota found in seawater and oyster flesh.

365

In situ microbial dynamics during POMS
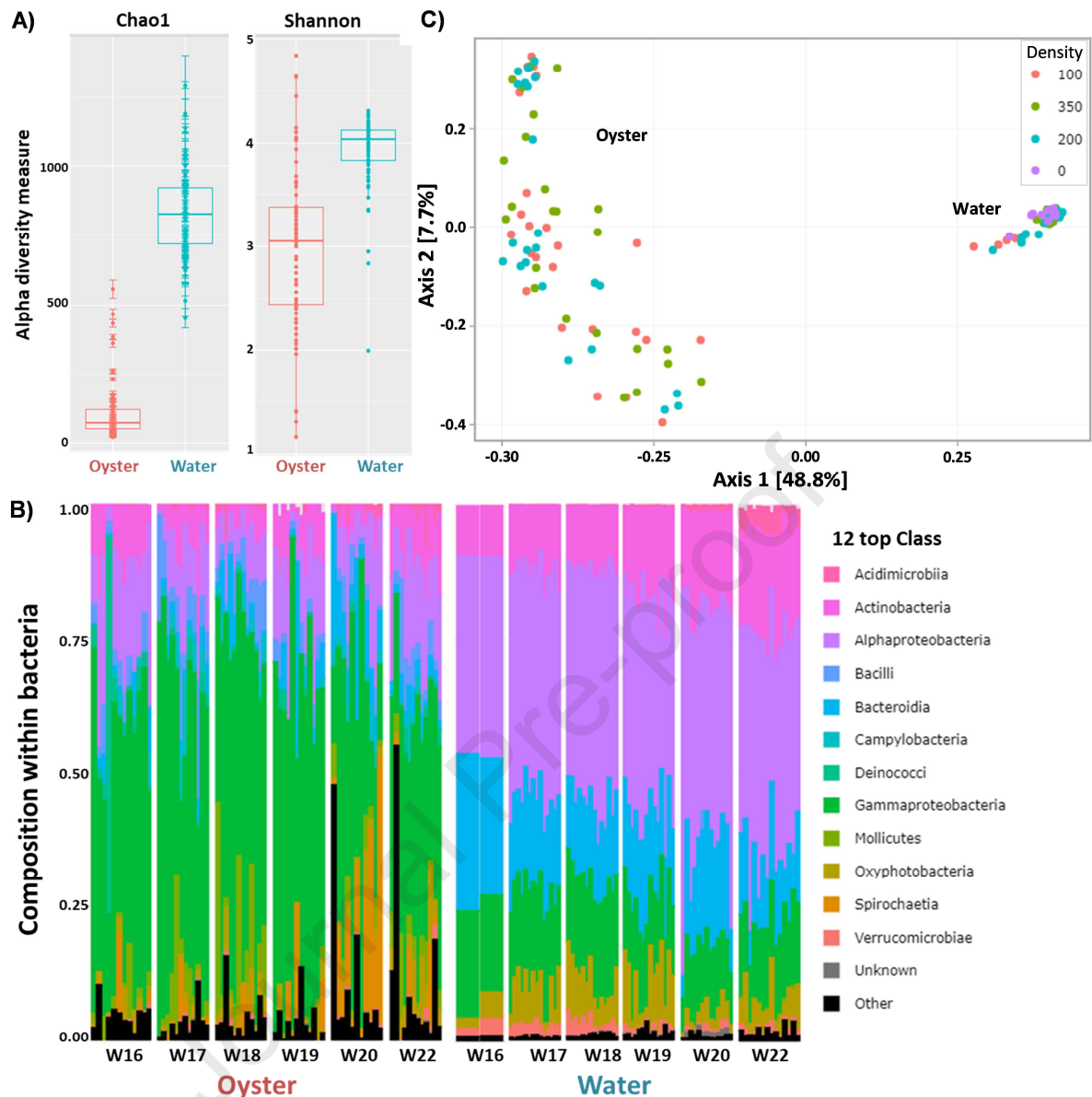
Figure 5: Bacterial microbiota analyses: A) Box plots of alpha diversity (Chao1 and Shannon) indices observed in water and oyster flesh, B) Principal coordinate analysis (PCoA) plot of the Bray-Curtis dissimilarity matrix comparing oyster flesh and water samples whatever the oyster density (100, 200, 350) and C) Composition of bacterial communities observed in oyster flesh and in water according to sampling weeks (W16: 13–19th of April, W17: 20–26th of April, W18: 27 April-3rd of May, W19: 4–10th of May, W20: 11–17th of May and W22: 25–31st of May 2015). The axes of the PCoA represent the two synthetic variables that explained the most variation of the dataset.

20

375

376   Bacterial communities were analysed and identified at the genera level (Figure 6) during

377   the POMS episode. The most significant changes in bacterial communities occurred in oyster

378   flesh where several bacterial taxa increased in relative abundance at the onset of mortality

379   (Figure 6, oyster, clusters I and II). Some genera appeared in W17 during the "starting period"

380   (e.g. *Vibrio* to *Bacteroidia* Figure 5 Cluster I and *Flavobacterium* to *Sulfurovum,* Figure 6,

381   oyster, Cluster II) whereas others increased in W18 during the "moribund peak"

382   (*Marinifilacea*, *Psychrilyobacter, Arcobacter and Psychrobium* Figure 6, oyster, cluster I),

383   just before the mortality peak in W19 during which Bacteroides, *Clostridiales* and *Saprospira*

384   were observed (Figure 6, oyster, cluster I).
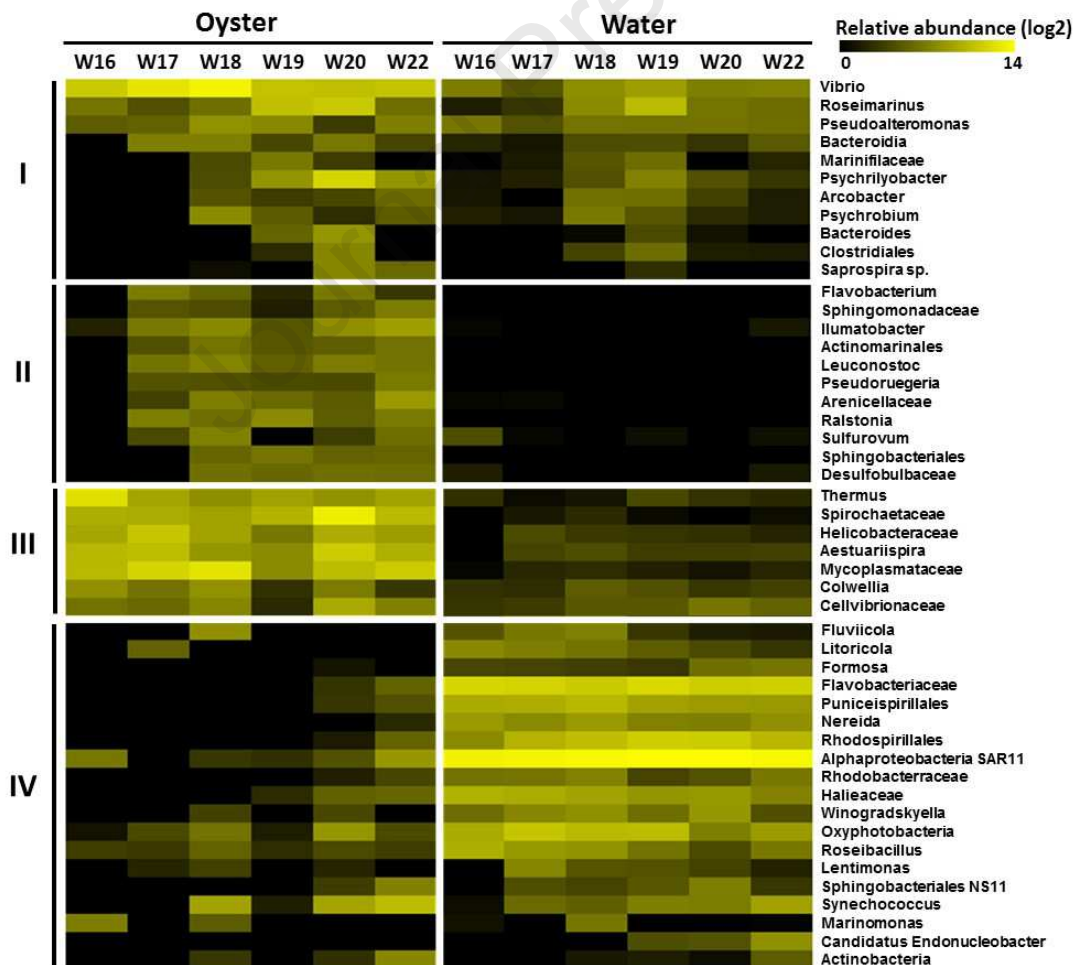
385

386   Figure 6: Heatmap of the bacterial genera that significantly changed in relative abundance

387   during the *in-situ* POMS episode. Frequencies are given for oyster flesh (left part) and for the

388   water column (right part). Sampling weeks are the same as in Fig. 3. Only genera with a

389   relative proportion > 5% in at least one sample are shown. The intensity level of the yellow

390   represents the relative abundance of bacterial taxa.

391

392   Interestingly, some of the bacteria (cluster I) were also found in the surrounding water

393   during the moribund and/or mortality peaks. Higher relative abundances of the opportunistic

394   bacterial genera (*Vibrio, Roseimarinus, Bacteroidia, Marinifilacea, Psychrilyobacter,*

395   *Arcobacter, Psychrobium, Bacteroides, Clostridiales* and *Saprospira*) were observed in the

396   water column during the moribund and mortality periods (Figure 6, Water, Cluster I).

397

398   **4. Discussion**

399   Pacific Oyster Mortality Syndromes have been reported worldwide and have devastated

400   Pacific oyster (*Crassostrea gigas*) juveniles (Garcia et al., 2011; Mineur et al., 2014; Pernet et

401   al., 2012, 2014a; Segarra et al., 2010). This study is the first to simultaneously describe the

402   dynamics of OsHV-1 loads over time and changes in the microbiota community in oyster

403   flesh *in-situ*, and to document the release of OsHV-1 and opportunistic bacteria from oysters

404   into the water column during a mortality event.

405

406   *4.1. Temporal dynamics of oyster flesh microbiota*

407   The 54% mortality rate of oyster juveniles recorded in the Thau lagoon from April to May

408   2015 occurred during the same time period as all the other POMS events that have occurred

409   every year since 2008 (Pernet et al., 2014b, 2012, 2010; Richard et al., 2019), when the water

410   temperature rises to 17 °C (Pernet et al., 2012). The oyster densities observed were not found

411   to have an effect either on the mortality rate, or on herpesvirus dynamics, or on changes in the

412   community of bacteria in oyster flesh. It would be interesting to confirm this result with

413   higher densities (i) at the scale of the lantern, knowing that oyster farmers can introduce up to

414   600 individuals per storey, but also (ii) at the scale of the culture tables in the Thau lagoon

415   (see Figure 2 in Gangnery et al. 2003), where oysters can be reared at a maximum density of 3

416   million juveniles per 500 m² table. OsHV-1 DNA was detected in the flesh of the oysters

417   during the POMS episode. Viral load ranges were comparable to those quantified in oyster

418   flesh during mortality events in France (Pernet et al., 2014b, 2012; Renault et al., 2014), or

419   Australia (Paul-Pont et al., 2014, 2013; Whittington et al., 2015b). OsHV-1 DNA was

420   detected in oyster flesh one week before the first visual symptoms of infection, i.e.,

421   dysfunction of valve closure at emersion. The temporal dynamics of the OsHV-1 DNA

422   quantified in oyster flesh could be compared to a Gaussian curve, as already shown for pools

423   of infected oyster juveniles (Richard et al., 2017; D. Schikorski et al., 2011). The phase during

424   which increases were observed may correspond to the replication phase of OsHV-1, thereby

425   compromising the oyster immune system and subsequently leading to bacteraemia and

426   mortality (de Lorgeril et al., 2018b). The descending phase corresponds to periods during

427   which effective control of viral replication is achieved in surviving oysters, as previously

428   observed for oyster juveniles (He et al., 2015). A shift in oyster microbiota in favour of

429   opportunistic bacteria such as *Vibrio, Arcobacter*, *Psychrobium and Psychrilyobacter,* all

430   previously found to be associated with oyster mortality (de Lorgeril et al., 2018b, 2018a; Lasa

431   et al., 2019; Le Roux et al., 2016; Lokmer and Mathias Wegner, 2015), was also observed

432   during the POMS episode. As already observed using an experimental infection approach (de

433   Lorgeril et al., 2018b), these results confirmed *in-situ* that disease in juvenile oysters arises

In situ microbial dynamics during POMS

434 from infection involving OsHV-1 and a shift in oyster microbiota in favour of opportunistic

435 bacteria.

436

437 *4.2. Release of pathogens from oysters into the water column*

438 Although the herpes virus is around 70-80 nm in size (Renault et al., 1994, 2000),

439 protocols used for conditioning and sampling were unable to detect OsHV-1 DNA in the free

440 form in water filtered at < 0.22 µm. By contrast, OsHV-1 DNA combined with suspended

441 matter was detected in the proximity of oyster lanterns in shellfish farms. This suspended

442 matter may correspond to living and non-living particles, but currently, we have no

443 information concerning their size class (pico, nano, microplankton), the composition of the

444 particles (organic, mineral) or their type (procaryotes, eucaryotes). Indeed, we do not know

445 whether OsHV-1 was associated with any type of suspended matter or whether the OsHV-1

446 was associated with dead oyster tissue and/or organisms involved in their decomposition

447 (bacteria, heterotrophic flagellates, ciliates) whose abundance increased during the mortality

448 episode (Richard et al. 2019). Further studies are thus required to investigate the association

449 of OsHV-1 with particles in the water column to better understand the fate of OsHV-1 and its

450 life cycle in marine environments.

451 The structure of the bacterial community in oyster flesh differed significantly from that

452 observed in the water column in terms of alpha and beta diversity, with a higher alpha

453 diversity in the water than in the oysters, as previously reported by Lokmer et al. (2016).

454 These differences were associated with the dominance of *Gammaproteobacteria* in oyster

455 flesh vs. *Alphaproteobacteria, Actinobacteria* and *Bacteroidia* in water samples. These results

456 are in agreement with those of Pujalte et al. (1999) and Lokmer et al. (2016), who observed

457 dominance of *Alphaproteobacteria* in water.

In situ microbial dynamics during POMS

458   This study is original in that it used an *in-situ* approach and pelagic chambers to enable

459   observation of pathogen dynamics in oysters and in the water column during an episode of

460   POMS *in situ*. As observed in laboratory experiments (Evans et al., 2016; Sauvage et al.,

461   2009; D. Schikorski et al., 2011), we confirmed that the OsHV-1 load in the water column

462   increased in proximity to infected oysters. Release of OsHV-1 started one week before the

463   first clinical symptoms were observed and reached maximum values (23,251 $_{C9C10}$ copies.ml^{-1})

464   when the moribund rate was highest (32 ± 3%). During this "moribund phase", 2 billion viral

465   particles were released per hour and per oyster lantern into the water column. Release of

466   OsHV-1 correlated with the OsHV-1 load observed in oyster flesh, suggesting that moribund

467   and dead infected oysters are major sources of the virus, as suggested by Sauvage et al.

468   (2009). In addition to the release of OsHV-1, we also describe an increase in the occurrence

469   of several genera of bacteria in the surrounding water during incubation in pelagic chambers

470   in the presence of oysters. These included *Vibrio, Roseimarinus, Psychrobium, Arcobacter,*

471   *Psychrilyobacter* and *Clostridiales*, all previously shown to be associated with oyster

472   mortality (Clerissi et al., 2020; de Lorgeril et al., 2018b; Lasa et al., 2019; Le Roux et al.,

473   2016; Lokmer and Mathias Wegner, 2015). The transfer of these opportunistic bacteria from

474   oysters into the water column reached maximum during the moribund phase and the mortality

475   peak.

476   An increase in the OsHV-1 load and in opportunistic pathogenic bacteria in the water

477   column may allow spread of the disease in the environment as suggested for OsHV-1 during

478   cohabitation experiments between infected and naïve oysters (Petton et al., 2015a, 2013; D.

479   Schikorski et al., 2011). Spread of the disease from infected to healthy oysters may be

480   favoured by hydrodynamic currents and connectivity, as previously suggested (Pernet et al.,

481   2014a, 2012) given that strong hydrodynamic connectivity has previously been observed

482   between shellfish farms in the Thau lagoon (Lagarde et al., 2019). Bearing in mind that

483   OsHV-1 and some of the opportunistic bacteria released into the environment are known to

484   cause diseases in other marine species (bivalves, holothurians, fish: Table 1), these transfers

485   of pathogens could cause mortality of larval or juvenile stages of other marine species during

486   POMS. The abundance of these species could thus decrease over time before the latter

487   disappear in the long term. Consequently, we hypothesise that the transfers of pathogens

488   could reduce marine biodiversity in ecosystems exploited by shellfish farming, particularly in

489   confined environments such as the Thau lagoon. The impact of these massive and recurrent

490   POMS events on other species, as well as the role of other ecological compartments on

491   disease spread now needs to be investigated in other types of ecosystems.

492

493   **5. Conclusion and perspectives**

494   This study demonstrated, for the first time in a natural environment, the successive release

495   of OsHV-1 and opportunistic bacteria from oysters into the water column during a 3-week

496   period, i.e., during a POMS episode. These viral and bacterial transfers into the water column

497   may favour the spread of disease between oysters within farms. Further analyses are required

498   to evaluate the effect of these pathogen releases on other marine organisms to determine the

499   consequences of massive oyster mortality on marine biodiversity in oyster growing

500   ecosystems.

In situ microbial dynamics during POMS

501

502   Table 1: A non-exhaustive list of different pathogens found to cause diseases in different marine species (see references) belonging to the list
503   of bacterial genera that were released into the water surrounding the suspended oyster lanterns during the mortality episode studied here.

Pathogen	Species	Host	Species	References
Virus	OsHV-1	European flat	*Ostrea edulis*	(Arzul et al., 2001; I Arzul et al., 2001; Mirella Da Silva et al., 2008)
	OsHV-1	Portuguese oyster	*Crassostrea angulata*	(I Arzul et al., 2001)
	OsHV-1	Suminoe oyster	*Crassostrea rivularis*	(I Arzul et al., 2001)
	OsHV-1	Manila clam	*Ruditapes philippinarum*	(Arzul et al., 2001)
	OsHV-1	carpet shell clam	*Ruditapes decussatus*	(Arzul et al., 2001)
	OsHV-1 µvar	French scallop	*Pecten maximus*	(Arzul et al., 2001)
Vibrio	*Vibrio alginolyticus and Vibrio splendidus*	Carpet shell clam	*Ruditapes decussatus*	(Gomez-Léon et al., 2005)
	V. anguillarum,V. alginolyticus,V. harveyi, V. splendidus	Seabream	*Sparus aurata*	(Balebona et al., 1998)
	Vibrio harveyi and V. splendidus	Shrimp	*Peneus monodon*	(Lavilla-Pitogo et al., 1990)
	Vibrio cyclitrophicus, V. splendidus, V. harveyi, V. tasmaniensis	Holothuria	*Apostichopus japonicus*	(Deng et al., 2009)
Arcobacter	*Vibrio & Arcobacter*	Mussel	Mytilus galloprovincialis	(Li et al., 2019)
	Arcobacter	Cod larvae	*Gadus morhua*	(Vestrum et al., 2018)

27

504 **Declaration of competing interest**

505 The authors declare no conflicts of interest

506

507 **CREdiT authorship contribution statement**

508 **Marion Richard:** Conceptualization, Methodology, Sampling, Resources, Formal

509 analysis, Visualization, Supervision, Project Administration, Funding Acquisition, Writing-

510 Original Draft, Writing – Review & Editing, **Jean Luc Rolland**, Resources, OsHV-1 DNA

511 analysis, Writing – Review & Editing, **Yannick Gueguen and Julien Delorgeril,** Resources,

512 microbiota analysis, Formal analysis, Visualization, Writing – Review & Editing, **Juliette**

513 **Pouzadoux,** microbiota analysis, Formal analysis, **Behzad Mostajir, Sebastien Mas,**

514 **Béatrice Bec,** Methodology, Resources and Writing – Review & Editing, **David Parin,**

515 Methodology, Resources, **Patrik Le Gall**, **Serge Mortreux**, **Grégory Messiaen and**

516 **Jocelyne Oheix,** Diving sampling, **Franck Lagarde, Emmanuelle Roque d'Orbcastel,**

517 Diving sampling, Writing – Review & Editing, **Martine Fortune, Annie Fiandrino,**

518 Sampling.

519

520 **Acknowledgments**

541

542   References

543   Arzul, I., Nicolas, J.L., Davison, A.J., Renault, T., 2001. French scallops: A new host for

544   ostreid herpesvirus-1. Virology 290, 342–349. https://doi.org/10.1006/viro.2001.1186

545   Arzul, I, Renault, T., Lipart, C., 2001. Experimental herpes-like viral infections in marine

546   bivalves: Demonstration of interspecies transmission. Dis. Aquat. Organ. 46, 1–6.

547   https://doi.org/10.3354/dao046001

548   Arzul, I., Renault, T., Lipart, C., Davison, A.J., 2001. Evidence for interspecies transmission

549   of oyster herpesvirus in marine bivalves 865–870.

550   Ausubel, F.M., Brent, R., Kingston, R.E., Moore, D.D., Seidman, J.G., Smith, J.A., Struhl, K.,

In situ microbial dynamics during POMS

551   2003. Preparation of genomic DNA from mammalian tissue, in: Sons, J.W.& (Ed.),

552   Current Protocol in Molecular Biology. Hoboken, NJ, USA, pp. 2.2.1-2.2.3.

553   Balebona, M.C., Zorrilla, I., Morinigo, M.A., Borrego, J.J., 1998. Survey of bacterial

554   pathologies affecting farmed gilt-head sea bream (*Sparus aurata* L .) in southwestern

555   Spain from 1990 to 1996. Aquaculture 19–35.

556   Carrasco, N., Gairin, I., Pérez, J., Andree, K.B., Roque, A., 2017. A Production Calendar

557   Based on Water Temperature , Spat Size , and Husbandry Practices Reduce OsHV-1 µ

558   var Impact on Cultured Pacific Oyster *Crassostrea gigas* in the Ebro Delta (Catalonia),

559   Mediterranean Coast of Spain 8, 1–10. https://doi.org/10.3389/fphys.2017.00125

560   Clarke, K.R., Warwick, R.M., 2001. Changes in Marine Communities: An Approach to

561   Statistical Analysis and Interpretation, 2nd Edition. PRIMER-E, Plymouth Marine

562   Laboratory, UK.

563   Clerissi, C., Lorgeril, J. De, Petton, B., Lucasson, A., Toulza, E., 2020. Microbiota

564   Composition and Evenness Predict Survival Rate of Oysters Confronted to Pacific

565   Oyster Mortality Syndrome. Front. Microbiol. 11, 1–11.

566   https://doi.org/10.3389/fmicb.2020.00311

567   Corporeau, C., Tamayo, D., Pernet, F., Quéré, C., Madec, S., 2014. Proteomic signatures of

568   the oyster metabolic response to herpesvirus OsHV-1 µVar infection. J. Proteomics 109,

569   176–187. https://doi.org/10.1016/j.jprot.2014.06.030

570   de Lorgeril, J., Escoubas, J.M., Loubiere, V., Pernet, F., Le Gall, P., Vergnes, A., Aujoulat, F.,

571   Jeannot, J.L., Jumas-Bilak, E., Got, P., Gueguen, Y., Destoumieux-Garzón, D., Bachère,

572   E., 2018a. Inefficient immune response is associated with microbial permissiveness in

573   juvenile oysters affected by mass mortalities on field. Fish Shellfish Immunol. 77, 156–

574   163. https://doi.org/10.1016/j.fsi.2018.03.027

In situ microbial dynamics during POMS

575   de Lorgeril, J., Lucasson, A., Petton, B., Toulza, E., Montagnani, C., Clerissi, C., Vidal-

576   Dupiol, J., Chaparro, C., Galinier, R., Escoubas, J.M., Haffner, P., Dégremont, L.,

577   Charrière, G.M., Lafont, M., Delort, A., Vergnes, A., Chiarello, M., Faury, N., Rubio, T.,

578   Leroy, M.A., Pérignon, A., Régler, D., Morga, B., Alunno-Bruscia, M., Boudry, P., Le

579   Roux, F., Destoumieux-Garzón, D., Gueguen, Y., Mitta, G., 2018b. Immune-suppression

580   by OsHV-1 viral infection causes fatal bacteraemia in Pacific oysters. Nat. Commun. 9.

581   https://doi.org/10.1038/s41467-018-06659-3

582   Deng, H., He, C., Zhou, Z., Liu, C., Tan, K., Wang, N., Jiang, B., Gao, X., Liu, W., 2009.

583   Isolation and pathogenicity of pathogens from skin ulceration disease and viscera

584   ejection syndrome of the sea cucumber Apostichopus japonicus. Aquaculture 287, 18–

585   27. https://doi.org/10.1016/j.aquaculture.2008.10.015

586   Escudié, F., Auer, L., Bernard, M., Mariadassou, M., Cauquil, L., Vidal, K., Maman, S.,

587   Hernandez-Raquet, G., Combes, S., Pascal, G., 2018. FROGS: Find, Rapidly, OTUs

588   with Galaxy Solution. Bioinformatics 34, 1287–1294.

589   https://doi.org/10.1093/bioinformatics/btx791

590   Evans, O., Hick, P., Whittington, R.J., 2016. Distribution of Ostreid herpesvirus-1 (OsHV-1)

591   microvariant in seawater in a recirculating aquaculture system. Aquaculture 458, 21–28.

592   https://doi.org/10.1016/j.aquaculture.2016.02.027

593   Gangnery, A., Chabirand, J-M, Lagarde, F., Le Gall, P., Oheix, J., Bacher, C., Buestel, D.

594   2003. Growth model of the Pacific oyster, *Crassostrea gigas*, cultured in Thau Lagoon

595   (Méditerranée, France). Aquaculture 215: 267–290.

596   Garcia, C., Thébault, A., Dégremont, L., Arzul, I., Miossec, L., Robert, M., Chollet, B.,

597   François, C., Joly, J.P., Ferrand, S., Kerdudou, N., Renault, T., 2011. Ostreid herpesvirus

598   1 detection and relationship with *Crassostrea gigas* spat mortality in France between

31

In situ microbial dynamics during POMS

599   1998 and 2006. Vet. Res. 42, 73. https://doi.org/10.1186/1297-9716-42-73

600   Gomez-Léon, J., Villamil, L., Lemos, M.L., Novoa, B., Figueras, A., 2005. Isolation of *Vibrio*

601   *alginolyticus* and *Vibrio splendidus* from Aquacultured Carpet Shell Clam (Ruditapes

602   decussatus) Larvae Associated with Mass Mortalities. Appl. Environ. Microbiol. 71, 98–

603   104. https://doi.org/10.1128/AEM.71.1.98

604   Green, T.J., Rolland, J.-L., Vergnes, A., Raftos, D., Montagnani, C., 2015. OsHV-1

605   countermeasures to the Pacific oyster's anti-viral response. Fish Shellfish Immunol. 47,

606   435–43. https://doi.org/10.1016/j.fsi.2015.09.025

607   Green, T.J., Vergnes, A., Montagnani, C., de Lorgeril, J., 2016. Distinct immune responses of

608   juvenile and adult oysters (*Crassostrea gigas*) to viral and bacterial infections. Vet. Res.

609   47, 72. https://doi.org/10.1186/s13567-016-0356-7

610   He, Y., Jouaux, A., Ford, S.E., Lelong, C., Sourdaine, P., Mathieu, M., Guo, X., 2015.

611   Transcriptome analysis reveals strong and complex antiviral response in a mollusc. Fish

612   Shellfish Immunol. 46, 131–144. https://doi.org/10.1016/j.fsi.2015.05.023

613   King, W.L., Jenkins, C., Seymour, J.R., Labbate, M., 2019. Oyster disease in a changing

614   environment: Decrypting the link between pathogen, microbiome and environment. Mar.

615   Environ. Res. 143, 124–140. https://doi.org/10.1016/j.marenvres.2018.11.007

616   Klindworth, A., Pruesse, E., Schweer, T., Peplies, J., Quast, C., Horn, M., Glöckner, F.O.,

617   2013. Evaluation of general 16S ribosomal RNA gene PCR primers for classical and

618   next-generation sequencing-based diversity studies. Nucleic Acids Res. 41, 1–11.

619   https://doi.org/10.1093/nar/gks808

620   Lafont, M., Petton, B., Vergnes, A., Pauletto, M., Segarra, A., Gourbal, B., Montagnani, C.,

621   2017. Long-lasting antiviral innate immune priming in the Lophotrochozoan Pacific

622   oyster *Crassostrea gigas*. Sci. Rep. 7, 1–14.

623   https://doi.org/https://doi.org/10.1038/s41598-017-13564-0

624   Lagarde, F., Fiandrino, A., Ubertini, M., Roque, E., Mortreux, S., Chiantella, C., Bec, B.,

625   Bonnet, D., Roques, C., Bernard, I., Richard, M., Guyondet, T., Pouvreau, S., Lett, C.,

626   2019. Duality of trophic supply and hydrodynamic connectivity drives spatial patterns of

627   Pacific oyster recruitment. Mar. Ecolgy Prog. Ser. 632, 81–100.

628   Lasa, A., di Cesare, A., Tassistro, G., Borello, A., Gualdi, S., Furones, D., Carrasco, N.,

629   Cheslett, D., Brechon, A., Paillard, C., Bidault, A., Pernet, F., Canesi, L., Edomi, P.,

630   Pallavicini, A., Pruzzo, C., Vezzulli, L., 2019. Dynamics of the Pacific oyster pathobiota

631   during mortality episodes in Europe assessed by 16S rRNA gene profiling and a new

632   target enrichment next-generation sequencing strategy. Environ. Microbiol. 00.

633   https://doi.org/10.1111/1462-2920.14750

634   Lavilla-Pitogo, C.R., Baticados, M.C.L., Cruz-Lacierda, E.R., de la Pena, L.D., 1990.

635   Occurrence of luminous bacterial disease of *Penaeus monodon* larvae in the Philippines.

636   Aquaculture 91, 1–13. https://doi.org/10.1016/0044-8486(90)90173-K

637   Le Roux, F., Wegner, K., Polz, M., 2016. Oysters and Vibrios as a Model for Disease

638   Dynamics in Wild Animals. Trends Microbiol. 24, 568–580. https://doi.org/DOI:

639   10.1016/j.tim.2016.03.006

640   Li, Y.-F., Xu, J.-K., Chen, Y.-W., Ding, W.-Y., Shao, A.-Q., Liang, X., Zhu, Y.-T., Yang, J.-

641   L., 2019. Characterization of Gut Microbiome in the Mussel *Mytilus galloprovincialis* in

642   Response to Thermal Stress. Front. Physiol. 10, 1–9.

643   https://doi.org/10.3389/fphys.2019.01086

644   Lokmer, A., Kuenzel, S., Baines, J.F., Wegner, K.M., 2016. The role of tissue-specific

645   microbiota in initial establishment success of Pacific oysters. Environ. Microbiol. 18,

In situ microbial dynamics during POMS

646   970–987. https://doi.org/10.1111/1462-2920.13163

647   Lokmer, A., Mathias Wegner, K., 2015. Hemolymph microbiome of Pacific oysters in

648   response to temperature, temperature stress and infection. ISME J. 9, 670–682.

649   https://doi.org/10.1038/ismej.2014.160

650   Love, M.I., Huber, W., Anders, S., 2014. Moderated estimation of fold change and dispersion

651   for RNA-seq data with DESeq2. Genome Biol. 15, 1–21. https://doi.org/10.1186/s13059-

652   014-0550-8

653   Magoč, T., Salzberg, S.L., 2011. FLASH: Fast length adjustment of short reads to improve

654   genome assemblies. Bioinformatics 27, 2957–2963.

655   https://doi.org/10.1093/bioinformatics/btr507

656   Mahé, F., Rognes, T., Quince, C., de Vargas, C., Dunthorn, M., 2014. Swarm: Robust and fast

657   clustering method for amplicon-based studies. PeerJ 2014, 1–13.

658   https://doi.org/10.7717/peerj.593

659   Martin, M., 2011. Cutadapt removes adpter sequences from high-throuhput sequencing reads.

660   Tech. notes 17, 10–12.

661   McMurdie, P.J., Holmes, S., 2013. Phyloseq: An R Package for Reproducible Interactive

662   Analysis and Graphics of Microbiome Census Data. PLoS One 8.

663   https://doi.org/10.1371/journal.pone.0061217

664   Mineur, F., Provan, J., Arnott, G., 2014. Phylogeographical analyses of shellfish viruses:

665   inferring a geographical origin for ostreid herpesviruses OsHV-1 (Malacoherpesviridae).

666   Mar. Biol. 162, 181–192. https://doi.org/10.1007/s00227-014-2566-8

667   Mirella Da Silva, P., Renault, T., Fuentes, J., Villalba, A., 2008. Herpesvirus infection in

668   European flat oysters *Ostrea edulis* obtained from brood stocks of various geographic

In situ microbial dynamics during POMS

669   origins and grown in Galicia (NW Spain). Dis. Aquat. Organ. 78, 181–188.

670   https://doi.org/10.3354/dao01874

671   Paul-Pont, I., Dhand, N.K., Whittington, R.J., 2013. Influence of husbandry practices on

672   OsHV-1 associated mortality of Pacific oysters *Crassostrea gigas*. Aquaculture 412–

673   413, 202–214. https://doi.org/10.1016/j.aquaculture.2013.07.038

674   Paul-Pont, I., Evans, O., Dhand, N.K., Rubio, A., Coad, P., Whittington, R.J., 2014.

675   Descriptive epidemiology of mass mortality due to Ostreid herpesvirus-1 (OsHV-1) in

676   commercially farmed Pacific oysters (*Crassostrea gigas*) in the Hawkesbury River

677   estuary, Australia. Aquaculture 422–423, 146–159.

678   https://doi.org/10.1016/j.aquaculture.2013.12.009

679   Pépin, J.F., Riou, A., Renault, T., 2008. Rapid and sensitive detection of ostreid herpesvirus 1

680   in oyster samples by real-time PCR. J. Virol. Methods 149, 269–76.

681   https://doi.org/10.1016/j.jviromet.2008.01.022

682   Pernet, F., Barret, J., Le Gall, P., Corporeau, C., Dégremont, L., Lagarde, F., Pépin, J.F.,

683   Keck, N., 2012. Mass mortalities of Pacific oysters *Crassostrea gigas* reflect infectious

684   diseases and vary with farming practices in the Mediterranean Thau lagoon, France.

685   Aquac. Environ. Interact. 2, 215–237. https://doi.org/10.3354/aei00041

686   Pernet, F., Barret, J., Marty, C., Moal, J., Gall, P. Le, Boudry, P., 2010. Environmental

687   anomalies, energetic reserves and fatty acid modifications in oysters coincide with an

688   exceptional mortality event. Mar. Ecol. Prog. Ser. 401, 129–146.

689   https://doi.org/10.3354/meps08407

690   Pernet, F., Lagarde, F., Jeanné, N., Daigle, G., Barret, J., Le Gall, P., Quere, C., Roque

691   d'orbcastel, E.R., 2014a. Spatial and temporal dynamics of mass mortalities in oysters is

692   influenced by energetic reserves and food quality. PLoS One 9.

In situ microbial dynamics during POMS

693   https://doi.org/10.1371/journal.pone.0088469

694   Pernet, F., Lagarde, F., Le Gall, P., Roque d'Orbcastel, E., 2014b. Associations between

695   farming practices and disease mortality of Pacific oyster *Crassostrea gigas* in a

696   Mediterranean lagoon. Aquac. Environ. Interact. 5, 99–106.

697   https://doi.org/10.3354/aei00096

698   Petton, B., Boudry, P., Alunno-Bruscia, M., Pernet, F., 2015a. Factors influencing disease-

699   induced mortality of Pacific oysters *Crassostrea gigas*. Aquac. Environ. Interact. 6, 205–

700   222. https://doi.org/10.3354/aei00125

701   Petton, B., Bruto, M., James, A., Labreuche, Y., Alunno-Bruscia, M., Le Roux, F., 2015b.

702   Crassostrea gigas mortality in France: The usual suspect, a herpes virus, may not be the

703   killer in this polymicrobial opportunistic disease. Front. Microbiol. 6, 1–10.

704   https://doi.org/10.3389/fmicb.2015.00686

705   Petton, B., Pernet, F., Robert, R., Boudry, P., 2013. Temperature influence on pathogen

706   transmission and subsequent mortalities in juvenile Pacific oysters *Crassostrea gigas*.

707   Aquac. Environ. Interact. 3, 257–273. https://doi.org/10.3354/aei00070

708   Pujalte, M.J., Ortigosa, M., Macián, M.C., Garay, E., 1999. Aerobic and facultative anaerobic

709   heterotrophic bacteria associated to Mediterranean oysters and seawater. Int. Microbiol.

710   2, 259–266. https://doi.org/10.2436/im.v2i4.9224

711   Renault, T., Bouquet, A.L., Maurice, J.-T., Lupo, C., Blachier, P., 2014. Ostreid Herpesvirus

712   1 Infection among Pacific Oyster (*Crassostrea gigas*) Spat: Relevance of Water

713   Temperature to Virus Replication and Circulation Prior to the Onset of Mortality. Appl.

714   Environ. Microbiol. 80, 5419–5426. https://doi.org/10.1128/aem.00484-14

715   Renault, T., Cochennec, N., Le Deuff, R.M., Chollet, B., 1994. Herpes-like virus infecting

716   japanese oyster (*Crassostrea gigas*). Bull. Eur. Ass. Fish. Pathol 14, 64–66.

717   Renault, T., Le Deuff, R.M., Chollet, B., Cochennec, N., Gerard, A., 2000. Concomitant

718   herpes-like virus infections in hatchery-reared larvae and nursery-cultured spat

719   *Crassostrea gigas* and *Ostrea edulis*. Dis. Aquat. Organ. 42, 173–183.

720   https://doi.org/10.3354/dao042173

721   Richard, M., Bec, B., Vanhuysse, C., Mas, S., Parin, D., Chantalat, C., Le, P., Fiandrino, A.,

722   Lagarde, F., Mortreux, S., Ouisse, V., Luc, J., Degut, A., Hatey, E., Fortune, M., Roque,

723   E., Messiaen, G., Munaron, D., Callier, M., Oheix, J., Derolez, V., Mostajir, B., 2019.

724   Changes in planktonic microbial components in interaction with juvenile oysters during a

725   mortality episode in the Thau lagoon (France). Aquaculture 503, 231–241.

726   https://doi.org/10.1016/j.aquaculture.2018.12.082

727   Richard, M., Bourreau, J., Montagnani, C., Ouisse, V., Gall, P. Le, Fortune, M., Munaron, D.,

728   Messiaen, G., Callier, M.D., Roque, E., 2017. Influence of OsHV-1 oyster mortality

729   episode on dissolved inorganic fluxes : An ex situ experiment at the individual scale.

730   Aquaculture 475, 40–51. https://doi.org/10.1016/j.aquaculture.2017.03.026

731   Rognes, T., Flouri, T., Nichols, B., Quince, C., Mahé, F., 2016. VSEARCH: A versatile open

732   source tool for metagenomics. PeerJ 2016, 1–22. https://doi.org/10.7717/peerj.2584

733   Sauvage, C., Pépin, J.F., Lapègue, S., Boudry, P., Renault, T., 2009. Ostreid herpes virus 1

734   infection in families of the Pacific oyster, *Crassostrea gigas*, during a summer mortality

735   outbreak: Differences in viral DNA detection and quantification using real-time PCR.

736   Virus Res. 142, 181–187. https://doi.org/10.1016/j.virusres.2009.02.013

737   Schikorski, D., Faury, N., Pepin, J.F., Saulnier, D., Tourbiez, D., Renault, T., 2011.

738   Experimental ostreid herpesvirus 1 infection of the Pacific oyster *Crassostrea gigas*:

739   Kinetics of virus DNA detection by q-PCR in seawater and in oyster samples. Virus Res.

155, 28–34. https://doi.org/10.1016/j.virusres.2010.07.031

Schikorski, David, Renault, T., Saulnier, D., Faury, N., Moreau, P., Pépin, J.F., 2011.

Experimental infection of Pacific oyster *Crassostrea gigas* spat by ostreid herpesvirus 1:

Demonstration of oyster spat susceptibility. Vet. Res. 42, 27.

https://doi.org/10.1186/1297-9716-42-27

Segarra, A., Pépin, J.F., Arzul, I., Morga, B., Faury, N., Renault, T., 2010. Detection and

description of a particular Ostreid herpesvirus 1 genotype associated with massive

mortality outbreaks of Pacific oysters, *Crassostrea gigas*, in France in 2008. Virus Res.

153, 92–99. https://doi.org/10.1016/j.virusres.2010.07.011

Tamayo, D., Corporeau, C., Petton, B., Quere, C., Pernet, F., 2014. Physiological changes in

Pacific oyster *Crassostrea gigas* exposed to the herpesvirus OsHV-1µVar. Aquaculture

432, 304–310. https://doi.org/10.1016/j.aquaculture.2014.05.023

Vestrum, R.I., Attramadal, K.J.K., Winge, P., Li, K., Olsen, Y., Bones, A.M., Vadstein, O.,

Bakke, I., 2018. Rearing water treatment induces microbial selection influencing the

microbiota and pathogen associated transcripts of Cod (*Gadus morhua*) Larvae. Front.

Microbiol. 9, 1–13. https://doi.org/10.3389/fmicb.2018.00851

Whittington, R.J., Dhand, N.K., Evans, O., Paul-Pont, I., 2015a. Further observations on the

influence of husbandry practices on OsHV-1 µVar mortality in Pacific oysters

Crassostrea gigas: Age, cultivation structures and growing height. Aquaculture 438, 82–

97. https://doi.org/10.1016/j.aquaculture.2014.12.040

Whittington, R.J., Hick, P.M., Evans, O., Rubio, A., Alford, B., Dhand, N., Paul-Pont, I.,

2015b. Protection of Pacific oyster (*Crassostrea gigas*) spat from mortality due to ostreid

herpesvirus 1 (OsHV-1 µVar) using simple treatments of incoming seawater in land-

based upwellers. Aquaculture 437, 10–20.

In situ microbial dynamics during POMS

764 https://doi.org/10.1016/j.aquaculture.2014.11.016

765

In situ microbial dynamics during POMS

HIGHLIGHTS:

- An increase in OsHV-1 and opportunistic bacterial pathogens occurs in oyster flesh during a

POMS outbreak

- OsHV-1 and opportunistic bacteria are released, in succession, into surrounding water

- Viral and bacterial pathogen release was at a maximum during the moribund and mortality
phases of the outbreak

Declaration of interests

☒ The authors declare that they have no known competing financial interests or personal relationships that could have appeared to influence the work reported in this paper.

☐The authors declare the following financial interests/personal relationships which may be considered as potential competing interests: